Scientific Bulletin of the
Politehnica University of Timisoara
Transactions on Mechanics Special issue

The International Conference on
Hydraulic Machinery and Equipments
Timisoara, Romania, October 16-17, 2008

Numerical and experimental investigations of the flow into an inducer

Liviu ANTON
Department of Hydraulic Machinery
"Politehnica" University of Timisoara
Bv Mihai Viteazu 1, 300223, Timisoara, Romania
Tel.: (+40) 256 403692, Fax: (+40) 256 403700,
Email: liviu.anton@mh.mec.upt.ro

Adrian STUPARU*
Department of Hydraulic Machinery
"Politehnica" University of Timisoara
Bv Mihai Viteazu 1, 300223, Timisoara, Romania
Tel.: (+40) 256 403692, Fax: (+40) 256 403700,
Email: astuparu@mh.mec.upt.ro

Alexandru BAYA
Department of Hydraulic Machinery
"Politehnica" University of Timisoara
Bv Mihai Viteazu 1, 300223, Timisoara, Romania
Tel.: (+40) 256 403692, Fax: (+40) 256 403700,
Email: abaya@mh.mec.upt.ro

***Corresponding author*: Bv. Mihai Viteazu 1, 300223, Timisoara, Romania**
Tel.: (+40) 256 403692, Fax: (+40) 256 403700, Email: astuparu@mh.mec.upt.ro

ABSTRACT

This paper presents the 2D and 3D numerical investigation of the turbulent flow in an inducer by using commercial code FLUENT 6.3. First the inducer is presented and then both equations that govern the flow and the boundary conditions imposed on the computational domain. The numerical results of the turbulent flow are validated with the experimental data.

KEYWORDS

numerical simulation, turbulent flow, pump inducer, flow analyse

NOMENCLATURE

t/l	[-]	space/chord ratio
p	[Pa]	pressure
v	[m/s]	absolute velocity
w	[m/s]	relative velocity
Q	[m^3/s]	flow rate
β_s	[º]	stager angle
β_o	[º]	inflow angle
β_2	[º]	outflow angle
c_p	[-]	pressure coefficient
g	[m/s^2]	gravity
ρ	[kg/m^3]	density
s	[mm]	thickness
RSM		Reynolds Stress Model
PS		pressure side
SS		suction side
n_b		number of blades

INTRODUCTION

The inducer is an axial impeller which is installed on the same shaft with the impeller of the pump, in front of it. The main goal of the inducer is generating an additionally specific energy on the inlet of the impeller of the pump. Consequently it prevents or reduces the cavitation. In the case of using an inducer with a pumping head of H_{ind}, the level of the minimum pressure from the impeller of the pump is rising in correspondence with this pumping head.

From figure 1, one may observe that the minimum pressure in a point *M* rises from $p_{\min}$ to $p_{\min c}$ if an inducer is used. That is why is important that the pumping head produced by the inducer, H_{ind}, to be as high as possible. This is realised by the optimum design of the geometry of the inducer.

The inducer is used usually for the pumps with severe suction condition and it has a "sacrificial role". It will be replaced after a certain operating time and that is why the technology for its execution has to be simple and economical.

For the classical inducers the hydrofoil cascade for the blades consists of straight hydrofoils with constant thickness like in figure 2. The blades of these inducers are materialised by a ruled surface generated by a straight line disposed on a circular propeller with constant slope and it is always perpendicular on the axis of the impeller.

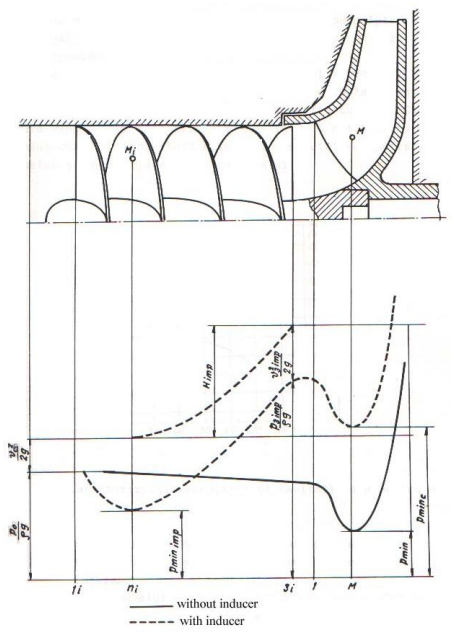

Figure 1. The effect of an inducer mounted on the shaft of a pump

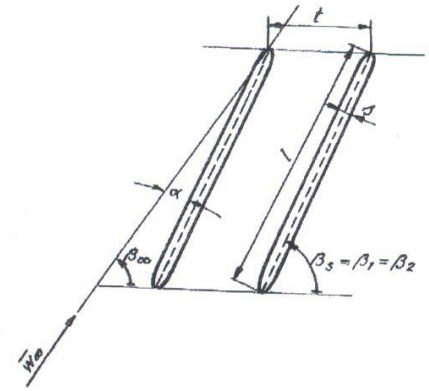

Figure 2. Straight hydrofoil of constant thickness for blade of the inducer

In conclusion, the usual inducer is like a screw.

Using the design equations for the turbo machinery blades, it is obtaining o slight curved shape for the camber line of the hydrofoil with better hydrodynamic conditions for the flow. This solution is difficult to manufacture from the technological point of view.

Tacking into consideration the influence of the outflow angle β_2 on the theoretical pumping head, which shows the raising of the pumping head with increasing of the angle β_2, in this paper it is proposed and investigated a straight hydrofoil cascade. This cascade has the stagger angle β_s equal with the angle β_2 of the curved hydrofoil cascade resulted from the designing condition computation. This type of the inducer will operate at nominal discharge with high angle of attack on the inlet. As a result, it will present bad cavitational behaviour. It is recommended that this type of inducer to be used to higher discharge than the nominal operating points, where the cavitational coefficient $NPSH_r$ has higher values.

The investigated inducer has two blades and is designed with straight hydrofoil cascade and rounded leading and trailing edge, see figure 3.

Figure 3. The inducer investigated experimental and numerical

The geometrical characteristic of the hydrofoil corresponding to the middle radius of the blade and the investigated operating condition are given in table 1:

Table 1. Geometrical characteristic and operating conditions of the investigated hydrofoil of the inducer

Q [m^3/s]	n [rpm]	s [mm]	β_s [°]	β_0 [°]	t/l [-]
0.336	1450	9	36.5	17.9	0.804

2D NUMERICAL INVESTIGATION OF THE FLOW IN THE INDUCER

The 2D flow simulation is performed because this is the basis for the classical designing method of an inducer.

The computational domain, figure 4, was generated using the pre-processor GAMBIT from FLUENT, based on the existing geometry.

The structured mesh for the 2D computational domain is generated with 60,000 cells. A boundary layer was attached to the hydrofoil in order to be able to compute the flow near a solid wall.

Figure 4. 2D computational domain of the inducer

The periodic boundaries of the domain are positioned at a distance, regarding the chord, equal with the space of the cascade, while the inlet is positioned at a distance equal with half of the space of the cascade and the outlet at a distance equal with four times the space of the cascade.

For the flow analysis presented in this paper we consider a 2D turbulent flow model. A steady relative flow is computed in the computational domain,

$$\nabla \cdot \vec{v} = 0 \tag{1}$$

$$\frac{d\left(\rho\vec{v}\right)}{dt} = \rho g - \nabla p + \mu\Delta\vec{v} \tag{2}$$

The numerical solution of flow equations (1) and (2) is obtained with the expert code FLUENT 6.3, using a Reynolds-averaged Navier-Stokes (RANS) solver. As a result, the viscosity coefficient is written as a sum of molecular viscosity μ and turbulent viscosity μ_T, and the last term in the right-hand-side of (1) becomes $\nabla\cdot\left[\left(\mu+\mu_T\right)\nabla\vec{V}\right]$. For steady, absolute flow the left hand side of (1) reduces $\nabla\cdot\left(\rho\vec{V}\vec{V}\right)$

We imposed on the inlet section of the 2D computational domain the two components of the relative velocity, corresponding to the prescribed flow rate and flow angle, together with the turbulence parameters, a turbulent intensity of 1% and a hydraulic diameter of 0.3 m.

$$w_x = \frac{Q}{S_{IN}} = 4.757 \text{ m/s} \tag{3}$$

$$w_y = \frac{w_x}{tg\beta_0} = 14.728 \text{ m/s} \tag{4}$$

On the outlet section of the computational domain a radial equilibrium condition is chosen.

On the periodic surfaces of the domains the periodicity of the velocity, pressure and turbulence parameters were imposed.

The remaining boundary conditions for the domain correspond to zero relative velocity.

Based on our previous research work, the turbulent viscosity is computed using the RSM model.

The pressure coefficient is calculated with the following relation:

$$c_p = \frac{p - p_{IN}}{\frac{\rho}{2} w_{IN}^2} \tag{5}$$

For the validation of the numerical results, a comparison between the pressure coefficient obtained from the 2D numerical investigation and from experimental investigation is made, figure 5.

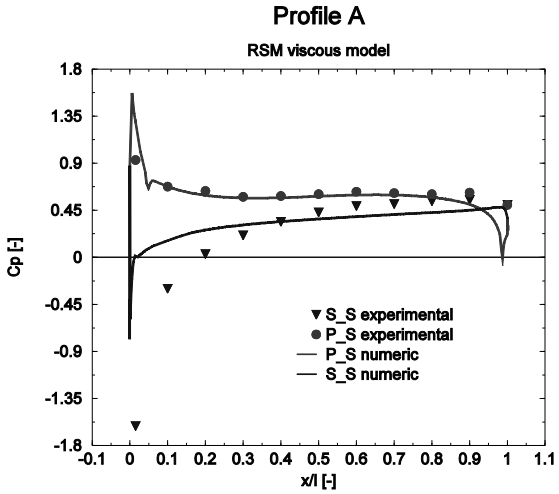

Figure 5. Pressure coefficient distribution along the blade of the inducer for 2D domain

For the 2D numerical simulation of the flow it can be observed that the pressure coefficient distribution along the pressure side of the blade is almost identical for the numerical simulation of the flow and the experimental investigation. For the suction side of the blade the distribution of the pressure coefficient is not alike for the numerical and experimental results because the detachment of the fluid from the hydrofoil.

In figure 6 and 7 the pattern of the 2D flow inside the inducer is presented with the help of the velocity distribution. It can be observed that on the suction side of the blade a detachment of the flow is present. This phenomenon appears due to the value of the flow angle which leads to the fact that the incidence point of the flow to be situated on the pressure side and not on the leading edge of the hydrofoil.

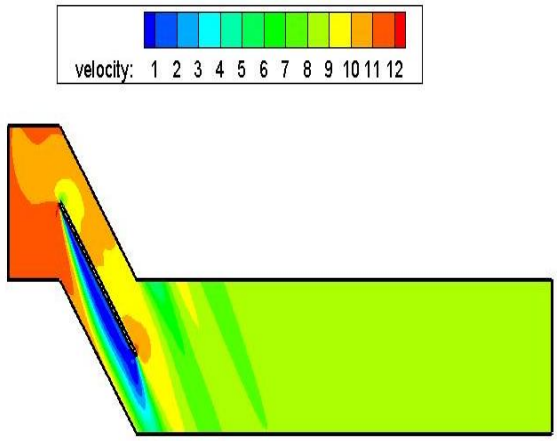

Figure 6. Velocity distribution inside the flow channel

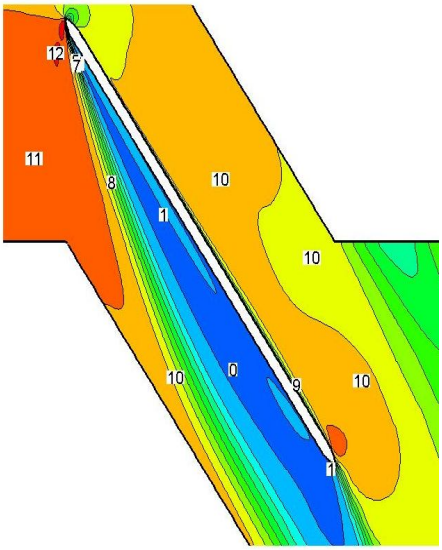

Figure 7. Velocity distribution near the hydrofoil

3D NUMERICAL INVESTIGATION OF THE FLOW IN THE INDUCER

The 3D numerical flow analyses is performed because of the limitations of the 2D method in the investigation of the real flow inside an inducer.

For the 3D turbulent flow simulation we solve a relative flow, in a rotating frame of reference with angular speed $\vec{\omega} = \omega\vec{k}$ ($\vec{k}$ being the unit vector of the inducer axis direction).

By introducing the relative velocity

$$\vec{w} = \vec{v} - \vec{\omega} \times \vec{r} \tag{6}$$

with $\vec{r}$ the position vector, the left hand side of (2) becomes

$$\frac{\partial}{\partial t}(\rho\vec{w}) + \nabla \cdot (\rho\vec{w}\vec{w}) + 2\rho\vec{\omega} \times \vec{w} + \\ + \rho\vec{\omega} \times (\vec{\omega} \times \vec{r}) + \rho\frac{\partial\vec{\omega}}{\partial t} \times r \tag{7}$$

An important assumption used in the present computation is that ***the relative flow is steady***. This simplifies (2) by removing the first and last terms, and also allows the computation of flow on a single inter-blade channel.

The generated mesh for the 3D computational domain, figure 8, is structured and has 460,000 cells.

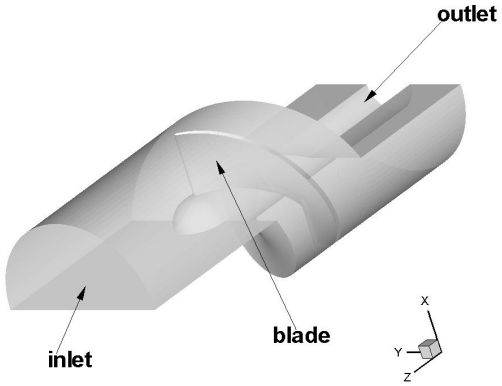

Figure 8. 3D computational domain of the inducer

For the inlet section of the 3D computational domain the velocity, corresponding to the prescribed discharge, together with the turbulence parameter, a turbulent intensity of 1% and a hydraulic diameter of 0.3 m, is imposed:

$$v = \frac{Q}{S_{IN}} = 4.757 \text{ m/s} \tag{8}$$

On the outlet section of the computational domain a radial equilibrium condition is chosen.

On the periodic surfaces of the domains the periodicity of the velocity, pressure and turbulence parameters were imposed.

$$\vec{v}(r,\theta,z) = \vec{v}\left(r,\theta + \frac{2\pi}{n_b}, z\right) \tag{9}$$

$$p(r,\theta,z) = p\left(r,\theta + \frac{2\pi}{n_b}, z\right) \tag{10}$$

The remaining boundary conditions for the domain correspond to zero relative velocity.

The same turbulence model, RSM, was used for the 3D numerical simulation of the turbulent flow.

The pressure coefficient is calculated with the following relation:

$$c_p = \frac{p - p_{IN}}{\frac{\rho}{2} v_{IN}^2} \qquad (10)$$

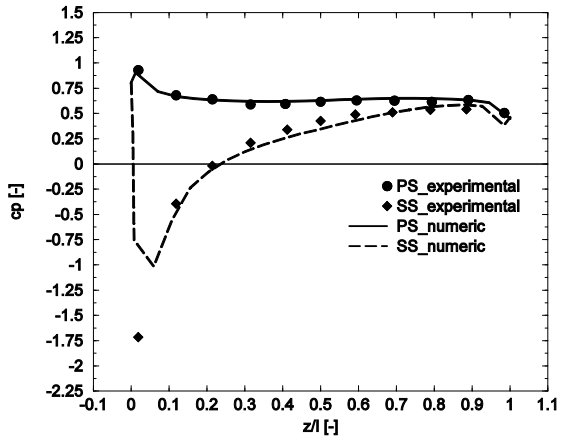

Figure 9. Pressure coefficient distribution along the blade of the inducer for 3D domain

From the comparison of the numerical and experimental pressure coefficient distribution along the pressure side, *PS*, and suction side, *SS*, of the blade, figure 9, it results a very good agreement for the 3D computational simulation of the flow. This proves that the turbulent model and boundary conditions were adequate chosen.

From the 3D numerical investigation of the flow inside the inducer it results the 3D effects due to the loading of the inducer blade which lead to the deviation of the stream trace towards the hub on the pressure side and towards the shroud on the suction side, figure 11. The flow on the pressure side towards the blade exit is positioned at the same radius as on the inlet of the blade. Moreover, the stream trace near to the pressure side moves near to the blade, while the stream trace on the suction side is pushed away from the blade, figure 12.

This type of phenomenon could not be determined with a 2D numerical investigation of the flow.

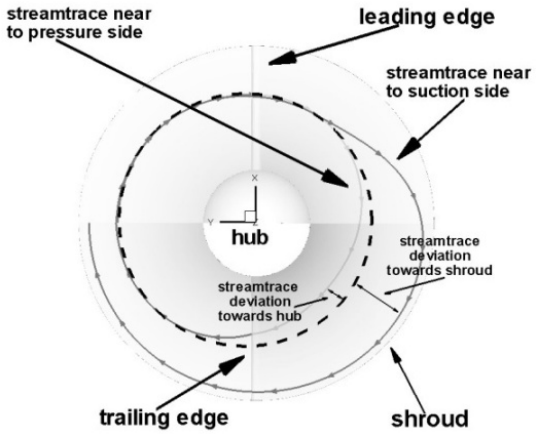

Figure 11. 3D effects on the loading of the inducer blades for stream trace

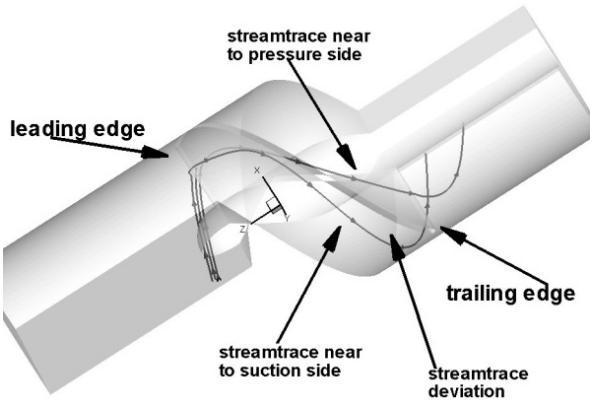

Figure 12. 3D deviation of the stream trace on the suction side

CONCLUSIONS

From the comparison of the numerical data with the experimental data regarding the pressure coefficient distribution along the blade of the inducer it results a good agreement. This proves that the boundary conditions and the RSM turbulence model were adequate chosen for both, 2D and 3D, numerical investigations.

The 2D numerical investigation of the flow inside the inducer predicts the presence of a dead zone of the flow on the suction side of the hydrofoil. This leads to the conclusion that the straight hydrofoil is not suited for the construction of the blade of the inducer.

The 3D full turbulent numerical investigation and analyse of the flow in an inducer reveals the 3D effects, that are presented due to the loading of the blade. Consequently the stream traces on the suction side are deviated towards the shroud and the stream traces on the pressure side are deviated towards the hub.

Because these 3D effects could not be taken into account in the design process of the inducer, it results a poor operation of this type of inducer.

The numerical investigation of the structure of the internal flow for this type of inducer leads to the conclusion that it is recommended the use of another type of hydrofoil cascade for manufacturing the blades of the inducer.

ACKNOWLEDGMENTS

Numerical computations have been performed at the Numerical Simulation and Parallel Computing Laboratory from the "Politehnica" University of Timisoara, National Center for Engineering of Systems with Complex Fluids.

REFERENCES

1. Anton, L. E. (1994). Determination of pressure distribution on the blades of an inducer, *Proceedings of XVII IAHR Symposium*, pp. 321-328, China, September, 1994, Beijing
2. Fluent Inc., (2001). *FLUENT 6.3 User's Guide*, Fluent Incorporated, Lebanon
3. Garay, P. N. (1996). *Pump Application Desk Book,* The Fairmont Press Inc., ISBN 0881732311
4. Mejri, I.; Bakir, F.; Rey, R. & Belamri, T. (2006). Comparison of Computational Results Obtained From a Homogeneous Cavitation Model With Experimental Investigations of Three Inducers. *Journals of Fluid Engineering*, Vol. 128, No. November 2006, 1308-1323
5. Susan-Resiga, R.; Muntean, S. (1999). Periodic boundary conditions implementation for the Finite Element Analysis of cascade flows, *Scientific bulletin of Politehnica University Timisoara*, Vol. 44(58), pp. 151-160
6. Anton, L.E., Milos, T., *Centrifugal pumps with inducer*, Ed. Orizonturi universitare, Timisoara,1998